

Computational Fluid Dynamics Model of the Heat Transfer at Thermal Resistance control of Building envelope

Vitalii Babak^a, Oleg Dekusha^a, Svitlana Kovtun^a, Zinaida Burova^b, Gleb Parkhomenko^a

^a General Energy Institute of NAS of Ukraine; 172, Antonovich str., 03150 Kyiv, Ukraine

^b National University of Life and Environmental Sciences of Ukraine, 15, Heroyiv Oborony str., 03041, Kyiv, Ukraine

Abstract

Nowadays, in the conditions of the need to save energy resources, it is no longer possible to simply increase the thermal and electrical power for the engineering needs of buildings. The way out from this situation is to insulate buildings. For monitoring thermal insulation and heat losses one of the main informative characteristics is thermal resistance. Experimental studies of the thermophysical characteristics of enclosed structures are defined in ISO 9869 standard. However, experimental studies have a number of significant drawbacks, among which the following should be highlighted: long duration of measurements and if necessary, the experiment can be extended; the need to use a large number of sensors to obtain a representative result; restrictions on climate parameters for conducting measurements. And also, a large number of influencing factors, such as the geometric dimensions and orientation of the building, the location of the sensors, external conditions, including weather during the tests, can lead to significant measurement errors. The proposed in work approach allows to reduce the influence of the above-mentioned factors in the process of determining thermal resistance and actual heat losses by creating a CFD model of object heat exchange. Subsequent verification of results showed that maximum deviation of the calculated and experimental data did not exceed 4%..

Keywords 1

Thermal Resistance, heat flux measurement, Computational Fluid Dynamics Model

1. Introduction

Nowadays, in the conditions of the need to save energy resources, it is no longer possible to simply increase the thermal and electrical power for the engineering needs of buildings. The way out from this situation is to insulate buildings, reduce transport heat losses and increase the efficiency of heat generating installations [1, 2].

It is considered that in order to save energy, it is advisable to insulate only those enclosing structures that have the maximum heat loss [3]. However, the inhomogeneity of the structures that arises in such cases can lead in the worst case to their deformation with the formation of cracks through which air and moisture from the environment will enter the structure. Also, cold bridges will form in the junctions of insulated and non-insulated areas, and moisture will condense [4]. Therefore, it is recommended to use complex external insulation of the entire building as a whole.

Along with traditional physical models and identification of parameters [5, 6], the use of methods for studying heat transfer using Computational Fluid Dynamics Model (CFD) modelling is increasing [7]. It is numerical simulation that expands the range of tasks to be solved, which are the basis for the creation of rational structures and the development of optimal operating modes [8]. CFD models for

Information Control Systems and Technologies (ICST-ODESSA-2023), September 21 - 23, 2023, Zaporizhzhia, Ukraine
EMAIL: vdoe@ukr.net (Vitalii Babak); olds@ukr.net (Oleg Dekusha); sveta_kovtun@ukr.net (Svitlana Kovtun); zinaburova@nubip.edu.ua (Zinaida Burova); tend.docs@gmail.com (Gleb Parkhomenko)

ORCID: 0000-0002-9066-4307 (Vitalii Babak); 0000-0003-3836-0485 (Oleg Dekusha); 0000-0002-6596-3460 (Svitlana Kovtun); 0000-0002-4712-6298 (Zinaida Burova); 0000-0003-0200-4892 (Gleb Parkhomenko)



© 2023 Copyright for this paper by its authors.

Use permitted under Creative Commons License Attribution 4.0 International (CC BY 4.0).



CEUR Workshop Proceedings (CEUR-WS.org) Proceedings

ventilation systems operating modes validation became one of the main tools [9, 10]. At the same time, the reliability and information content of the results of computational-theoretical and experimental studies increased [11].

For monitoring of the heat losses one of the main informative characteristics is thermal resistance [11]. Experimental studies of the thermophysical characteristics of enclosed structures are defined in ISO 9869 [12] standards. However, experimental studies have a number of significant drawbacks, among which the following should be highlighted: long duration of measurements (at least 72 hours), and if necessary, the experiment can be extended; the need to use a large number of sensors to obtain a representative result; restrictions on climate parameters for conducting measurements. And also a large number of influencing factors, such as the geometric dimensions and orientation of the building, the location of the sensors [13-15], external conditions, including weather during the tests, can lead to significant measurement errors [15].

The aim of the work is to reduce the influence of the above-mentioned factors in the process of determining actual heat losses by creating a CFD model of examined object accounting not only heat but air exchange, with subsequent verification of results, which is allows to increasing the accuracy of heat loss calculations.

2. Methodology and object of research

2.1. Research methodology

In accordance with the aim the following research methodology is proposed (Fig. 1).

Tests in natural conditions to determine the thermal resistance of building envelopes are performed when the heating systems are operating and, accordingly, there is a temperature difference on the examined building envelope.

At the initial stage, the analysis and determination the parameters of the room necessary for the experiment and simulation are carried out.

In the second step, the room is thermographed in accordance with ISO 6781 [16] to find a suitable location for the sensors to avoid thermal bridges, cracks or similar.

In the third step, heat flux and temperature sensors are mounted in accordance with the recommendations of ISO 9869-1 [12] and taking into account the results of thermography.

In the next step, tests are carried out in accordance with ISO 9869-1 [12]. Then, the results of the experiment for the first 24 hours are processed, and these data are input to the CFD model. After that, the experiment continues for at least another 48 hours in accordance with the recommendations of the standard and the results are processed.

The current values of the heat flux density q_i (W/m²) measured by the secondary measuring devices is calculated as a multiplication of measured signals of heat flux sensors E_i (mV) and their calibration coefficient K_{sensor} (W/(mV·m²)) by the formula:

$$q_i = K_{sensor} \cdot E_i, \quad (1)$$

According to the results of measuring the current values of heat flux q_i , the temperature of surfaces T_{i_i} and T_{e_i} , the air near them $T_{i_i}^{Air}$ and $T_{e_i}^{Air}$.

These values are averaged over a single full day (24 hours) or over several full days. For the averaged of the listed values, the arithmetic means of the current values of each quantity, measured at regular intervals, should be taken. Also, it is possible to apply wavelet analysis [17].

Next, for each zone calculated averaged measured values of such parameters:

- the temperature difference by the formula:

$$\Delta \bar{T}_{structure_n} = \bar{T}_{i_n} - \bar{T}_{e_n}; \quad (2)$$

where $n = 1, 2, \dots, N$;

- the temperature head by the formula:

$$\Delta \bar{T}^{Air} = \bar{T}_{i_n}^{Air} - \bar{T}_{e_n}^{Air}; \quad (3)$$

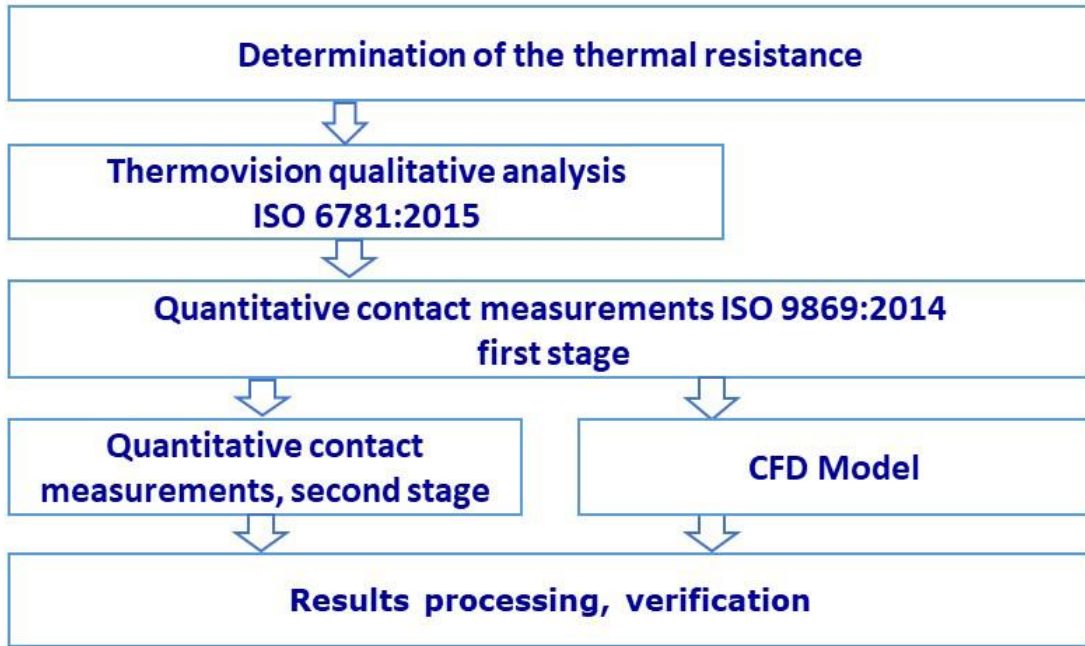


Figure 1: Flow chat of research methodology

- the temperature difference between the environment and the adjacent surface of the zone on the corresponding boundary layer, by the formulas:

$$\Delta \bar{T}_{internal_n} = \bar{T}_{i_n}^{Air} - \bar{T}_{i_n}, \quad (4)$$

$$\Delta \bar{T}_{external_n} = \bar{T}_{e_n} - \bar{T}_{e_n}^{Air}. \quad (5)$$

The average values of thermal resistance of the enclosing structures are calculated based on formulas (2) and (1):

$$\bar{R}_{structure_n} = \Delta \bar{T}_{structure_n} / \bar{q}_n, \quad (6)$$

At the same time, the CFD model is calculated. The distribution of temperature and heat fluxes is determined, and the parameters influencing the experiment are refined.

The next step is to verify the simulation based on the measurement results using the values of the corresponding temperatures and heat fluxes. Based on the data obtained, heat losses are calculated.

2.2. Experiment Description

The object of the study is a room 5.41 m long, 3.04 m wide and 3.2 m high. The thickness of the outer wall is 0.55 m, the window size is 2.1×2.0 m, the window thickness is 0.2 m, the thickness of the over-radiator section of the wall is 0.45 m, its width is 0.80 m, the width of the lateral vertical parts of the outer enclosing structure is 0.70 and 0.34 m.

In accordance with the developed methodology, thermography of the room was carried out. The results are shown in Fig. 2.

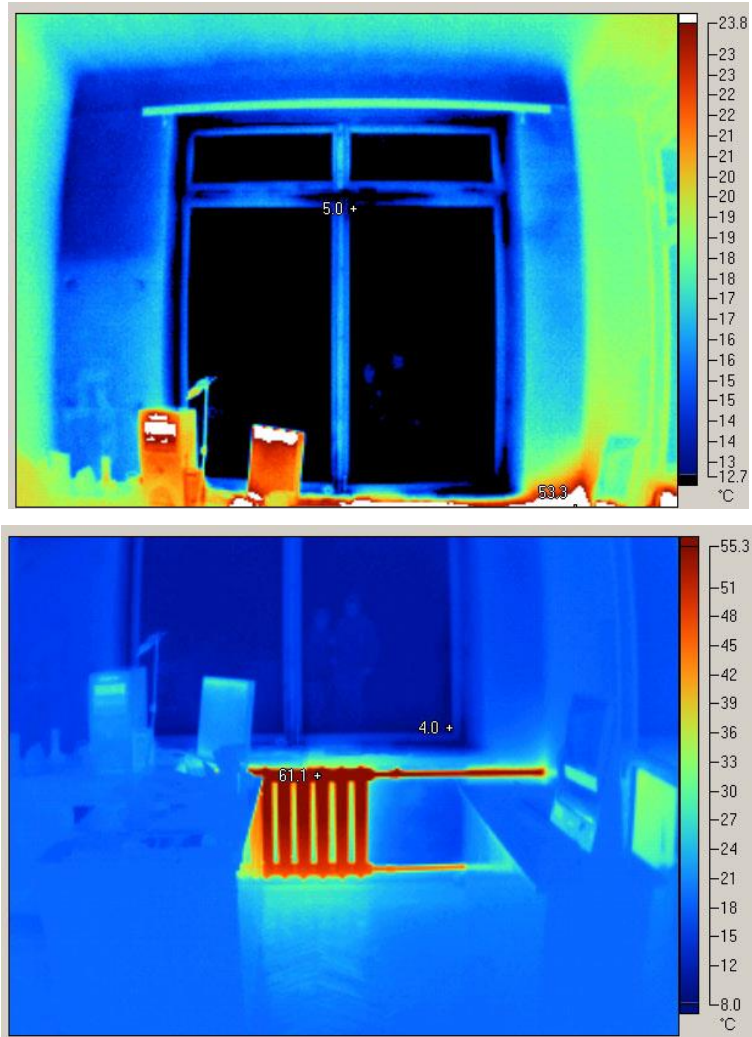


Figure 2: The results of thermography the inner surface of the outer wall of the investigated room
 Based on the results of thermography the inner surface of the outer wall of the studied room, the heat flux and temperature sensors were placed as shown in Fig. 3.



Figure 3: The heat flux and temperature sensor's location in the test room

Information-measuring system based on modules with 8-channel ADC with a bit of 16 bits and a conversion rate of 10 Hz, as temperature sensors used thermocouples with individual calibration in range -30 ... +100°C and absolute error ± 1 °C, heat flux sensor calibrated in range 1 ... 2000 W/m² with relative error 3 % [18,19].

Contact measurements are carried out with interval between channels 60s and in accordance with formulas 1–6, the signals from the sensors are processed. The results are shown in the Table 1.

Table 1

Experimental results

No	Parameter	Experimental results
1	Environment temperature, °C	-2
2	Air temperature in the room, °C	18.3
3	Inner surface of the room wall temperature, °C	15.6...16.4
4	Over-radiator section temperature, °C	32.8
5	Inner surface of the window temperature, °C	13.0
6	Radiator temperature, °C	50.8
7	Heat flux on the inner surface of the outer wall at point 1, W/m ²	25.7
8	Heat flux on the inner surface of the outer wall at point 2, W/m ²	20.8
9	Heat flux on the inner surface of the outer wall at point 3, W/m ²	13.8
10	Heat flux on the inner surface of the outer wall at point 4, W/m ²	11.7
11	Heat flux on the inner surface of the outer wall at point 5, W/m ²	47.6
12	Heat flux on the inner surface of the outer wall at point 6, W/m ²	46.9
13	Heat flux on the inner surface of the outer wall at point 7, W/m ²	13.8

Obtained experimental results on environment temperature and air temperature in the room indicates that requirements of ISO 9869[12] about temperature difference are met.

3. CFD model of the thermal state of the room

3.1. Model description

Computational fluid dynamics model created in STAR-CD software. In the model (Fig. 4), the conjugate heat exchange of the air inside the room with the heating system radiator is fixed. Heat exchange by radiation is applied by using the Discrete Beams model [8 ,9].

Emissivity of all surfaces inside the room was assumed to be 0.8, the radiator surface – 0.3 because of a number of radiator sections that re-radiate heat to each other and is necessary to reduce the radiant heat flux from the radiator in the model.

The air exchange with the environment simulated through the window slots 1 mm wide, as well as through the ventilation hole in the wall.

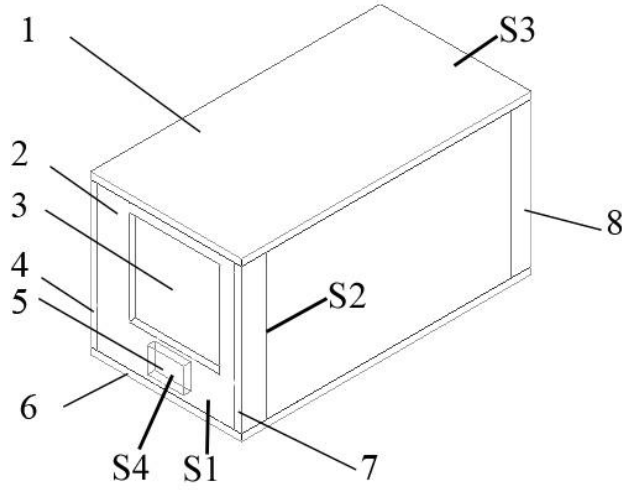


Figure 4: Scheme of the studied room from the inside: 1 - ceiling, 2 - outer wall, 3 - window, 4 - right side wall, 5 - radiator, 6 - floor, 7 - left side wall, 8 - inner wall

In the calculation for air, the model of an ideal incompressible gas with temperature-dependent thermophysical characteristics is accepted. In the model the thermal conductivity coefficient value for the outer wall was taken equal to 0.75 W/(m·K), for the window – 1.17 W/(m·K).

In the developed CFD model free convection caused by the action of the gravitational force applied. Justified and selected laminar air flow regime $Gr \cdot Pr = 9,55 \cdot 10^8$ [20]. The models contained about 350 thousand calculation cells. The system of energy equations for air and for solids (7) is solved in the conjugate formulation.

$$\varpi_x \frac{\partial T}{\partial x} + \varpi_y \frac{\partial T}{\partial y} + \varpi_z \frac{\partial T}{\partial z} = a \cdot \left(\frac{\partial^2 T}{\partial x^2} + \frac{\partial^2 T}{\partial y^2} + \frac{\partial^2 T}{\partial z^2} \right) \quad (7)$$

were ϖ_i – the fluid velocity vector projections onto the corresponding coordinate axis; T – temperature, °C; a – thermal diffusivity, m^2/c .

The conjugation condition for temperature and heat fluxes was set at the separation boundaries solid body–gas S2, S4 (see Fig.4). The equations of motion (8–10), and the continuity equation (11) are presented below.

$$\varpi_x \frac{\partial \varpi_x}{\partial x} + \varpi_y \frac{\partial \varpi_x}{\partial y} + \varpi_z \frac{\partial \varpi_x}{\partial z} = \nu \cdot \left(\frac{\partial^2 \varpi_x}{\partial x^2} + \frac{\partial^2 \varpi_x}{\partial y^2} + \frac{\partial^2 \varpi_x}{\partial z^2} \right) - \frac{1}{\rho} \cdot \frac{\partial p}{\partial x} \quad (8)$$

$$\varpi_x \frac{\partial \varpi_y}{\partial x} + \varpi_y \frac{\partial \varpi_y}{\partial y} + \varpi_z \frac{\partial \varpi_y}{\partial z} = \nu \cdot \left(\frac{\partial^2 \varpi_y}{\partial x^2} + \frac{\partial^2 \varpi_y}{\partial y^2} + \frac{\partial^2 \varpi_y}{\partial z^2} \right) - \frac{1}{\rho} \cdot \frac{\partial p}{\partial y} \quad (9)$$

$$\varpi_x \frac{\partial \varpi_z}{\partial x} + \varpi_y \frac{\partial \varpi_z}{\partial y} + \varpi_z \frac{\partial \varpi_z}{\partial z} = \nu \cdot \left(\frac{\partial^2 \varpi_z}{\partial x^2} + \frac{\partial^2 \varpi_z}{\partial y^2} + \frac{\partial^2 \varpi_z}{\partial z^2} \right) - \frac{1}{\rho} \cdot \frac{\partial p}{\partial z} - \frac{1}{\rho} \cdot \beta \cdot g_z \cdot \vartheta \quad (10)$$

were ν – kinematic viscosity coefficient of air, m^2/s ; ϖ – air velocity, m/s; p – pressure, Pa; β – volume expansion coefficient; ρ – air density, kg/m^3 ; $\vartheta = T - T_0$ – excess temperature, °C; T – fluid flow temperature, °C; T_0 – wall temperature, °C.

$$\frac{\partial \varpi_x}{\partial x} + \frac{\partial \varpi_y}{\partial y} + \frac{\partial \varpi_z}{\partial z} = 0 \quad (11)$$

were ϖ_i – the fluid velocity vector projections onto the corresponding coordinate axis.

On the outer wall outer boundary S1 (see Fig.4) boundary conditions of the III kind were set:

$$\alpha \cdot F \cdot (T_{S1} - T_{OC}) \Big|_{S1} = -\lambda \frac{\partial T}{\partial n} \Big|_{S1} \quad (12)$$

The conjugation conditions for temperature and heat fluxes at the interface S2, S4 (Fig.4) were set:

$$T|_{S2} = T^{Air}|, \quad Q|_{S2} = Q^{Air}|, \quad T|_{S5} = T|_B, \quad Q|_{S5} = Q^{Air}|, \quad (13)$$

If there is no heat exchange at the S3 boundary and the heat sink surface temperature is constant:

$$\frac{\partial T}{\partial n}|_{S3} = 0, \quad T|_{S4} = const, \quad (14)$$

were T_{OC} – environment temperature, °C, T_B – air temperature in the room, °C.

Convective-radiant heat transfer from the outer surface of the outer enclosing structure (outer wall) to the ambient air was determined by the empirical dependence [20]:

$$\alpha = 7,74 \cdot w_{Air}^{0,656} + 3,78 \cdot e^{-1,91 \cdot w_{Air}} + 5,67 \cdot \frac{\left(\frac{T_e}{100}\right)^4 - \left(\frac{T^{Air}}{100}\right)^4}{T_e - T^{Air}}, \quad (15)$$

were w_{air} – air velocity flowing around the outer surface of the outer wall is equal to 5 m/c, T_e – average temperature of the outer wall outer surface, °C, T^{Air} – environment temperature, °C.

Air exchange with the environment is carried out as follows: air with ambient (environment) temperature is supplied through the window opening into the testing room. As a result of heat exchange inside the room, the air warms up and is removed from the room through a vent hole in the wall opposite the outer one. The required air exchange rate was created due to the Velocity inlet boundary conditions with a given air velocity, as well as the direction of movement (perpendicular to the plane of the window and the vent hole).

3.2. The results of CFD modeling

As a results of CFD modeling the fields of temperature, heat flows and air movement speeds in the studied room were obtained.

In fig. 5 shows the velocity vectors in the inlet (a) and outlet (b) ventilation openings of the room under study.

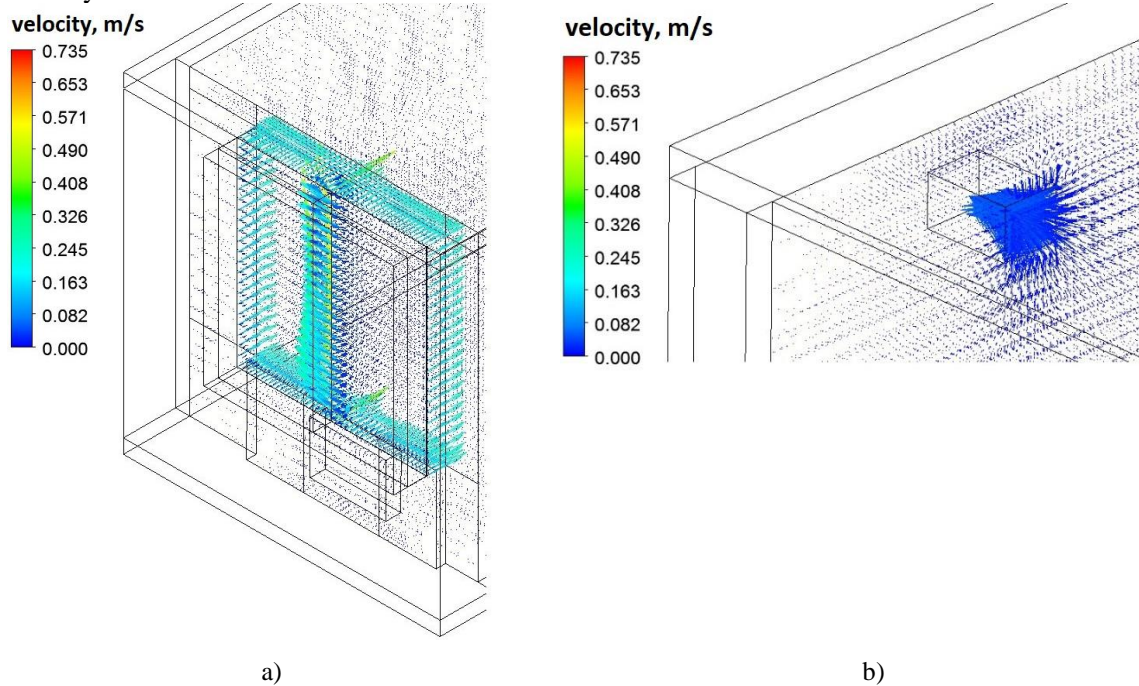


Figure 5: Air velocities distribution in the ventilation openings of the model: a) inlet in the window, b) outlet vent hole

The resulting heat flux field, shown in Fig. 6, is a confirmation of the significant uneven distribution of heat fluxes along the inner surface of the investigated room outer wall.

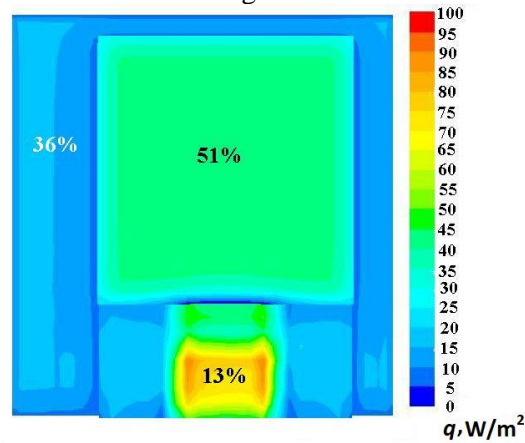


Figure 6: Heat flux distribution on the inner surface of the outer wall

As can be seen in Fig. 6 heat flux distribution on the outer wall surface is uneven. 36% of heat losses pass through the outer wall, excluding the surface of the radiator section, 13% through the over-radiator section, and 51% through the window surface.

Temperature distributions (Fig. 7) were obtained in different sections of the room, illustrating the unevenness of the temperature field

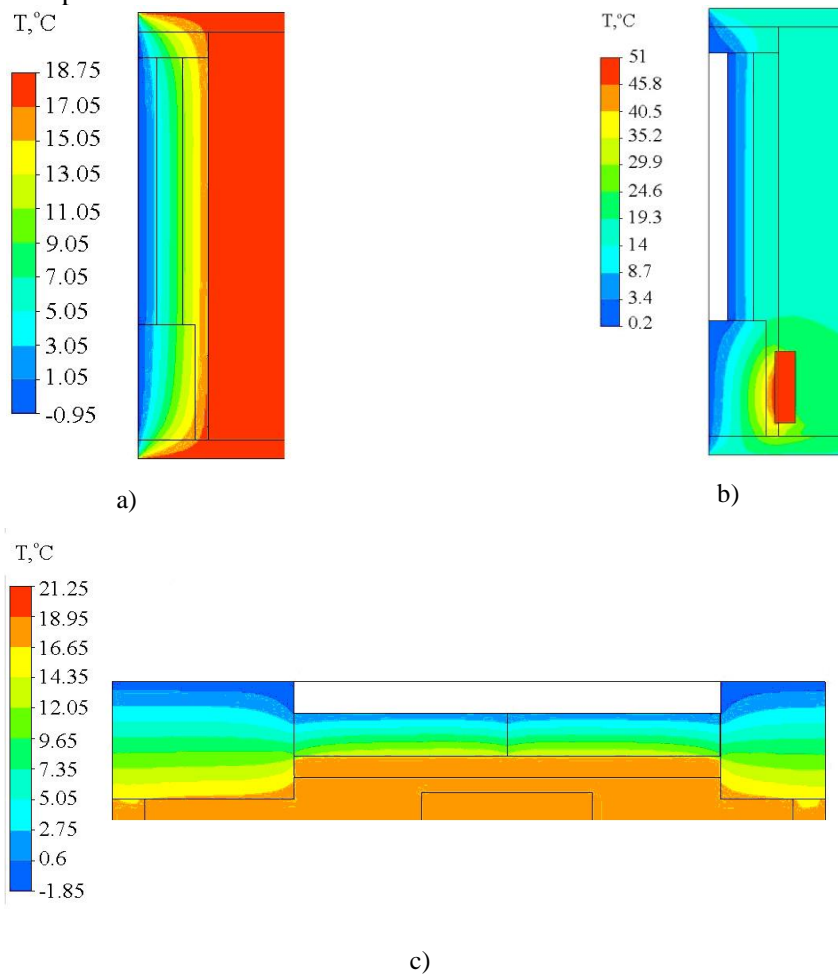


Figure 7: Temperature distribution in the enclosing structures of the test room: a) temperature field in the vertical section of the outer wall right side; b) temperature field in the central vertical section of the outer wall; c) temperature field in the horizontal section of the outer wall

4. Verification of the results

Verification of a three-dimensional model was carried out to determine the parameters of heat loss in rooms from the measured values of temperature and heat flux densities based on experimental data. The results are presented in Table 2.

As can be seen from Table 2, the maximum deviation of the calculated and experimental data did not exceed 4%.

After determining the thermal conductivity coefficients of the building envelope, the value of the air exchange rate is calculated based on the heat balance of the room.

Table 2

Values of measured and calculated temperatures and heat flux densities

No	Parameter	Measured results	Calculation results
1	Average air temperature in the room, °C	18.3	18.6
2	Inner surface of the room wall temperature, °C, at points (Fig.3)		
	point 2	15.6	15.6
	point 3	15.6	15.6
	point 4	16.4	16.2
3	Over-radiator section temperature, °C	32.8	33.1
4	Window surface temperature, °C	13.0	13.5
5	Heat flux on the inner surface of the outer wall at point 2, W/m ²	20.8	21.3
6	Heat flux on the inner surface of the outer wall at point 4, W/m ²	11.7	11.9
7	Heat flux on the inner surface of the outer wall at point 5, W/m ²	47.6	48.2

Individual components of the room heat balance – the values of heat flows through the enclosing structures of the room – are taken from the three-dimensional model and they are the heat losses of the test room. In the explored case the heat balance of the room can be described by the following formula:

$$Q_{RAD} = Q_{ew} + Q_{ow} + Q_{Air} \quad (16)$$

were Q_{RAD} – heat flux from the radiator; Q_{ew} – heat flux through the outer wall into the environment; Q_{ow} – heat flux through the window into the environment; Q_{Air} – heat flow with air exchange to the environment, which is calculated from the equation (16).

Then the air exchange rate in the test room can be calculated using the following equation:

$$m = \frac{Q_{Air}}{\rho \cdot C \cdot V \cdot (T_i^{Air} - T_{OC}^{Air})}, \quad (17)$$

were ρ – air density, kg/m³; C – air heat capacity, kJ/(kg·K); V – test room volume, m³; T_i^{Air} – average room temperature, °C; T_{OC}^{Air} – environment temperature, °C.

According to measurements, the air exchange rate was 0.75. The obtained values of thermal conductivity coefficients for the outer wall, window and air exchange rate make it possible to determine heat losses through individual enclosing structures of the room, as well as to develop solutions to reduce them.

The considered approach determined the values of heat losses through the outer wall, through the window and taking into account air exchange, which amounted to 190 W; 245W and 175W, respectively.

5. Conclusions

A proposed approach that allows to determine not only the thermal resistance, but also the heat losses of buildings, taking into account air exchange. A three-dimensional CFD model of the examined object heat exchange was built with accounting convective-radiant heat transfer.

Verification of a three-dimensional model was carried out to determine the parameters of heat losses in rooms from the measured values of temperature and heat flux densities based on experimental data. The error of the temperature and heat flux values obtained as a result of verification did not exceed 4% compared with the experimental data. The parameters of local heat losses were determined accounting air exchange.

Advantages of proposed approach are reduced influence of the subjective factor on the process of thermal resistance control of building envelope and ability to obtain distribution of the temperature and heat flux for each element construction. Also, possible to predict building envelope state and heat losses with accounting conductive and convective-radiant heat transfer in different environment conditions with use CFD model.

Limitation of proposed approach at the current state laying in using the steady state CFD model which means it is not full describe transition processes in building envelope. In the development of this work planned to create non-stationary CFD models in different software environments and compare results. As well, planned to variate the number calculation cells in CFD model and with extended verification for creating practical recommendations.

6. Acknowledgements

These researches have been performed within of the scientific program «Information technology for energy audit of buildings as a component of the energy security of the country».

7. References

- [1] V.P. Babak, L.M. Scherbak, Y.V. Kuts, A.O. Zaporozhets, Information and measurement technologies for solving problems of energy informatics. CEUR Workshop Proceedings, 3039, 2021, pp. 24–31. <http://ceur-ws.org/Vol-3039/short20.pdf>.
- [2] Final Energy Consumption by Sector. Report of the European Parliamentary Research Service. URL: <https://epthinktank.eu/2022/06/16/monitoring-the-energy-situation-in-the-eu-june-2022/final-energy-consumption-by-sector/>.
- [3] UNI/TS 11300-1: 2014 – Energy Performance of Buildings – Part 1: Determination of the Building Thermal Energy Demand for Climatization in Winter and Summer Season
- [4] G. Grazieschi, F. Asdrubali, G. Thomas, Embodied energy and carbon of building insulating materials: A critical review, *Cleaner Environmental Systems*, 2 (2021).
- [5] E. Sassine, Y. Cherif, E. Antczak, Parametric identification of thermophysical properties in masonry walls of buildings, 25 (2019).
- [6] P. De Wilde, The gap between predicted and measured energy performance of buildings: A framework for investigation. *Autom. Constr.*, 41 (2014) 40–49.
- [7] V. Peter, Nielsen Fifty years of CFD for room air distribution *Building and Environment*, 91 (2015) 78-90. doi:10.1016/j.buildenv.2015.02.035
- [8] B. Yang, A.K. Melikov, A. Kabanshi, C. Zhang, F.S. Bauman, G. Cao, H. Awbi, H. Wigö, J. Niu, K.W.D. Cheong, K.W. Tham, M. Sandberg, P.V. Nielsen, R. Kosonen, R. Yao, S. Kato, S.C. Sekhar, S. Schiavon, T. Karimipanah, X. Li, Z. Lin, A review of advanced air distribution methods - theory, practice, limitations and solutions, *Energy and Buildings*, 202 (2019). doi:10.1016/j.enbuild.2019.109359.
- [9] M. Hurnik, M. Blaszcok, Z. Popiolek, Air distribution measurement in a room with a sidewall jet: A 3D benchmark test for CFD validation, *Building and Environment*, 93 2 (2015). doi:10.1016/j.buildenv.2015.07.004.

- [10] Y. Wang, F.-Y. Zhao, J. Kuckelkorn, D. Liu, J. Liu, J.-L. Zhang, Classroom energy efficiency and air environment with displacement natural ventilation in a passive public school building, *Energy and Buildings*, 70 (2014) 258-270. doi:10.1016/j.enbuild.2013.11.071.
- [11] L. Evangelisti, C. Guattari, F. Asdrubali, Influence of heating systems on thermal transmittance evaluations: Simulations, experimental measurements and data post-processing, *Energy Build.* 168 (2018) 180-190. doi: 10.1016/j.enbuild.2018.03.032
- [12] ISO 9869-1, Thermal insulation–Building elements–In-situ measurement of thermal resistance and thermal transmittance–Part 1: Heat flow meter method, International Organization for Standardization, ISO, Geneva, Switzerland, 2014.
- [13] X. Meng, B. Yan, Y. Gao, J. Wang, W. Zhang, E. Long, Factors affecting the in situ measurement accuracy of the wall heat transfer coefficient using the heat flow meter method. *Energy Build.*, 86 (2015) 754–765. doi:10.1016/j.enbuild.2014.11.005
- [14] M. Cucumo, V. Ferraro, D. Kaliakatsos, M. Mele, On the distortion of thermal flux and of surface temperature induced by heat flux sensors positioned on the inner surface of buildings, *Energy Build.*, 158 (2018) 677–683. doi:10.1016/j.enbuild.2017.10.034
- [15] L. Evangelisti, C. Guattari, F. Asdrubali, Comparison between heat-flow meter and Air-Surface Temperature Ratio techniques for assembled panels thermal characterization, *Energy and Buildings*, 203 (2019) 109441. doi:10.1016/j.enbuild.2019.109441
- [16] ISO 6781-2015. Thermal performance of building – Qualitative detection of thermal irregularities in building envelopes – Infrared method, 2015.
- [17] O. Hotra, S. Kovtun, O. Dekusha, Ż. Grądz, V. Babak, J. Styczeń, Analysis of Low-Density Heat Flux Data by the Wavelet Method *Energies*, 16 1 (2023). doi: 10.3390/en16010430
- [18] V. Babak, O. Dekusha, S. Kovtun, S. Ivanov, Information-measuring system for monitoring thermal resistance. *CEUR Workshop Proceedings*, 2387, 2019, pp. 102-110. URL: <http://ceur-ws.org/Vol-2387/20190102.pdf>
- [19] O.L. Dekusha, S.I. Kovtun, V.V. Romanenko, S.V. Sozonov, Information-measuring Technology for Buildings Enclosing Structures Thermal Resistance Control *CEUR Workshop Proceedings*, 3309, 2022, pp. 301 – 313.
- [20] V.Y. Ledenev, I.V. Matveeva, Physico-technical basis of operation of external brick walls of civil buildings. TSTU, 2005.